Efficient Iris Segmentation using Grow-Cut Algorithm for Remotely Acquired Iris Images

Chun-Wei Tan, Ajay Kumar
Department of Computing, The Hong Kong Polytechnic University
Hung Hom, Kowloon, Hong Kong
cwtan@ieee.org, ajaykr@ieee.org

Abstract

This paper presents a computationally efficient iris segmentation approach for segmenting iris images acquired from at-a-distance and under less constrained imaging conditions. The proposed iris segmentation approach is developed based on the cellular automata which evolves using the Grow-Cut algorithm. The major advantage of the developed approach is its computational simplicity as compared to the prior iris segmentation approaches developed for the visible illumination iris segmentation images. The experimental results obtained from the three publicly available databases, i.e. UBIRIS.v2, FRGC and CASIA.v4-distance have respectively achieved average improvement of 34.8%, 31.5% and 31.4% in the average segmentation error, as compared to the recently proposed competing/best approaches. The experimental results presented in this paper clearly demonstrate the superiority of the developed iris segmentation approach, i.e., significant reduction in computational complexity while providing comparable segmentation performance, for the distantly acquired iris images.

1. Introduction

Robust automated human recognition based on distinctive physiological (face, fingerprint, hand, retina, etc.) or behavioral (gait, signature, voice, *etc*.) biometric characteristics has been getting more attention in order to provide reliable verification (1:1) or identification (1:N) of person. Many existing applications such as financial transaction, access control and border control involve the recognition process to ensure the identity and authenticity of a person. One of the typical examples is the largest national deployment of automatic iris recognition system in the United Arab Emirates (UAE) [1].

Iris recognition is one of the most promising biometric technologies which have been shown to be highly reliable and accurate. The uniqueness of each individual's iris is characterized by the rich texture patterns, which have been found to be stable throughout lifetime. In addition, the likelihood of two irises from the different persons is the same has been theoretically estimated to be 10^{-72} [20]. Iris is an overt body characteristic which makes it a suitable candidate to be used for *noninvasive* personal identification [5]. However, the existing iris recognition systems are constrained to work in a controlled environment and require full cooperation from the subjects to provide images within close distance (1–3 feet) [2, 16, 18]. Such rigidly imposed constraints are to ensure that the acquired iris images provide sufficient image quality to be employed for recognition (*i.e*. the acquired images are in focus and have minimum acceptable iris diameter [3, 4]). In addition, the existing iris recognition systems have quite limited applications and usually are designed to work in verification mode.

Recently, *remote* iris image acquisition using visible imaging has been attempted [6, 7, 23, 24] with much success and has been aimed to overcome several limitations of the conventional NIR (near infrared) based acquisition systems. The conventional NIR-based acquisition requires rigorous analysis and experiments in order to ensure the irradiance levels meeting the safety specifications [20-22]. In that sense, visible imaging iris acquisition seems to provide better option as it is less likely to be constrained by such specifications. The instinctive mechanism of the human eyes such as pupil dilation/contraction, blinking and aversion in response to the visible spectrum provides protection to our eyes from being injured by the excessive illumination level [7, 16, 18]. In addition, high resolution iris images can be conveniently acquired at-a-distance away from 3m with today's visible imaging technologies [16, 23, 24], which may facilitate the development of remote iris recognition for forensic and surveillance applications [7, 16]. However, the quality of the distantly acquired iris images using visible imaging is usually influenced by multiple noise sources. The commonly observed noises are as motion/defocus blur, occlusions from eyelashes, hair and eyeglasses, reflections, off-angle and partial eye images [10, 14, 16]. Therefore, development of robust iris segmentation approaches for the distantly acquired iris images using visible imaging has been gaining attention lately [8-18].

In [9], an integro-differential constellation model is employed to perform the iris segmentation. The algorithm uses multiple integro-differential operators [4], [19] to iteratively search for the local minimum score. This method provides sub-optimal solution in segmenting iris images

978-1-4673-1228-8/12/$31.00 ©2012 IEEE

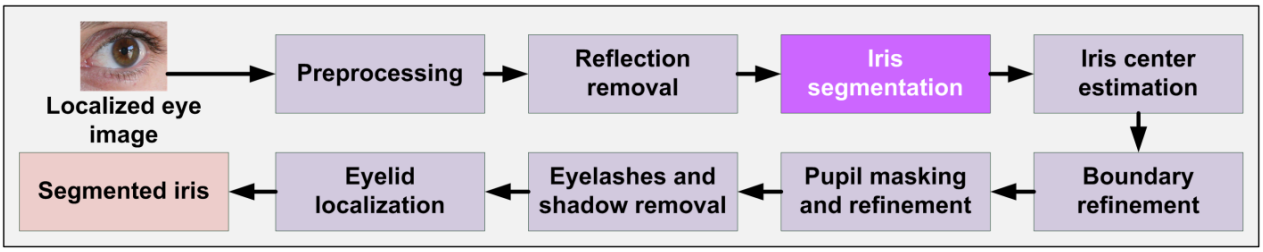

Figure 1: Block diagram of the developed iris segmentation approach.

and is still developed based on the conventional edge-based iris segmentation approach . The approach [8] trains neural network classifiers using colors as features to perform the iris segmentation. Image pixels are then classified into iris/non-iris category using the trained classifiers. Similarly, the approach [16] trains either neural network/support vector machine classifier by exploiting localized Zernike moments as features to classify image pixels into iris/non-iris category. Both of the approaches reported in [8, 16] require rigorous training of the classifiers and heavily computational cost is incurred in computing the image features.

1.1. Our work

This paper has developed a computationally efficient iris segmentation approach for segmenting iris images from the remotely acquired eye images. The proposed iris segmentation approach is based on the cellular automata which evolves using the Grow-Cut algorithm. The main advantages of the developed approach, as compared to the recent competing approaches [8, 9, 16], can be summarized as in the following:

- The main advantage of the developed approach lies in its *computational simplicity* which results in significantly reduction in computations since the computations of high-order moments is not required.
- The proposed approach does not require rigorous training from the use of neural network / support vector machine classifiers as employed in prior proposals.
- The proposed method achieves comparable segmentation performance. The experimental results obtained from the three publicly available databases, *i.e.* UBIRIS.v2 [7], FRGC [31-32] and CASIA.v4-distance [33] have respectively reported average improvement of 34.8%, 31.5% and 31.4% in the average segmentation error.

2. Iris segmentation

The block diagram of the proposed Grow-Cut based iris segmentation approach is shown in Figure 1. It is worth mentioning that the localized eye image is shown here are in color for better illustration and in actual implementation only the red channel of the color image is employed. Firstly, a Gaussian filter and a median filter are applied to the localized eye image I in order to mitigate the noise level

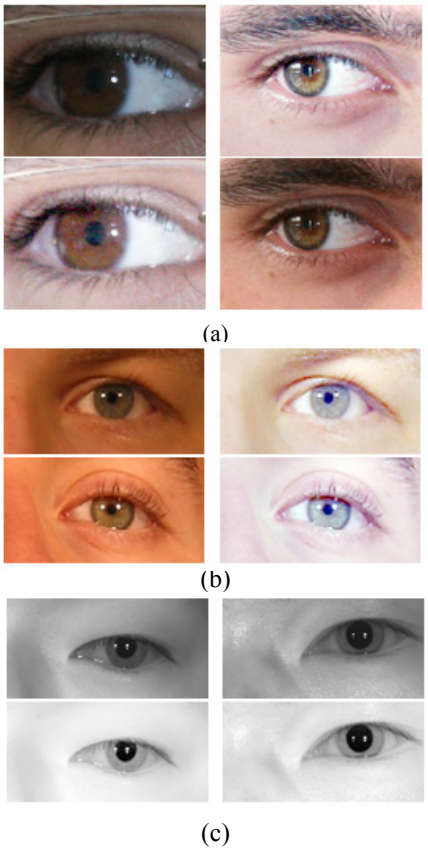

Figure 2: Image enhancement using Retinex algorithm for the three employed databases, (a) UBIRIS.v2, (b) FRGC, (c) CASIA.v4-distance. The top row shows the input images while the enhanced images are shown accordingly at the bottom row.

which is commonly affect observed for the images acquired in the unconstrained conditions. As similarly to [16], the image I is subject to further enhancement by applying Retinex algorithm [16, 25-27]. Figure 2 presents some sample of the Retinex enhanced images obtained from the.

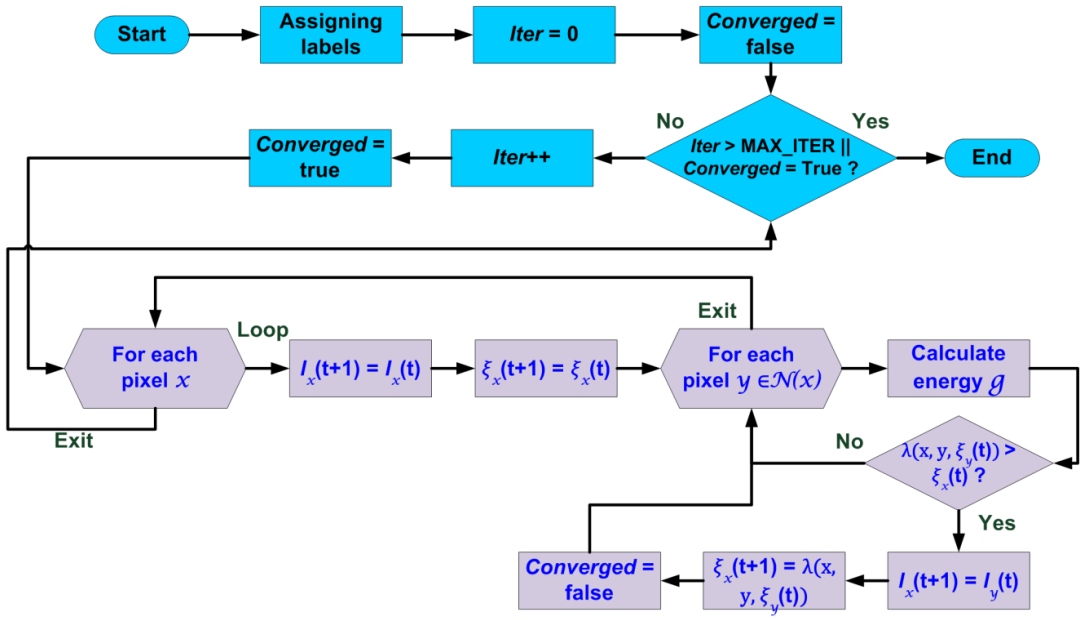

Figure 3: Flowchart of the proposed iris segmentation approach based on the Grow-Cut algorithm.

(a) (b)

Figure 4: Initial assignment of labels. (a) Input image, (b) Assigned labels (Cyan - foreground; Gray – background; Black - otherwise).

three employed databases. The reflection removal method in [16] is then employed to detect the reflection from the enhanced image $\tilde{I}$. The detected reflection region is filled by performing the interpolation in order to reduce the effect of those reflection pixels to the iris segmentation in the subsequent operation

The iris segmentation approach proposed in this work is developed based on the Grow-Cut (GC) algorithm [28], which models the image using cellular automata. The procedure of the proposed iris segmentation approach is illustrated using the flowchart as depicted in Figure 3. The GC algorithm requires initialization of seed points which provides the initial labels l to indicate the foreground (+1) and background (-1) (iris and non-iris) pixels, as illustrated in Figure 4. In order to facilitate such process, the following rules are employed:

$$l_k = \begin{cases} +1 & \text{if } g_k < mod(I) - \varphi_f \sigma(\tilde{I}), \\ -1 & \text{if } g_k > mod(I) - \varphi_b \sigma(\tilde{I}), \\ 0 & \text{Otherwise,} \end{cases} \quad (1)$$

where g_k denotes the intensity value at pixel k, $mod(\tilde{I})$ and $\sigma(\tilde{I})$ correspond to the mode and the standard deviation of the image $\tilde{I}$. The weights $\varphi_f = \{1.6,1.6,1.6\}$ and $\varphi_b = \{0.7,0.7,1.25\}$ which obtained from the training images are respectively set for the UBIRIS.v2, FRGC and CASIA.v4-distance databases. At each discrete time $t+1$, the pixel x may be experiencing a state transition (see Figure 3) based on the cost function λ, as defined as follows:

$$\lambda\left(x, y, \xi_y(t); y \in \mathcal{N}(x)\right) = \left(1 - \frac{\|g_x - g_y\|_2}{max\ \|g\|_2}\right)^{-} . \xi_y(t). \quad (2)$$

The $(.)^-$, $\mathcal{N}(x)$ and $\xi_y(t)$ are respectively denote the monotonous decreasing function, the neighborhood pixels of x and the energy of pixel y at time t. The label and the energy of pixel x are updated accordingly if the calculated λ is greater than $\xi_y(t)$. In other words, the image pixel which presents a higher cost λ is attempting to spread its influence to the neighborhood pixels. Such evolution process is iterated until it converges to a stable state or the predefined maximum iteration is reached. The GC segmented iris images are subject to further enhancement, which the robust post-processing operations (*iris center estimation, boundary refinement, pupil masking and refinement, eyelashes and shadow removal and eyelid localization*) as proposed in [16] are employed. Such post-processing operations can effectively mitigate the influence from noisy pixels such as eyelashes and shadow.

3. Experiments and Results

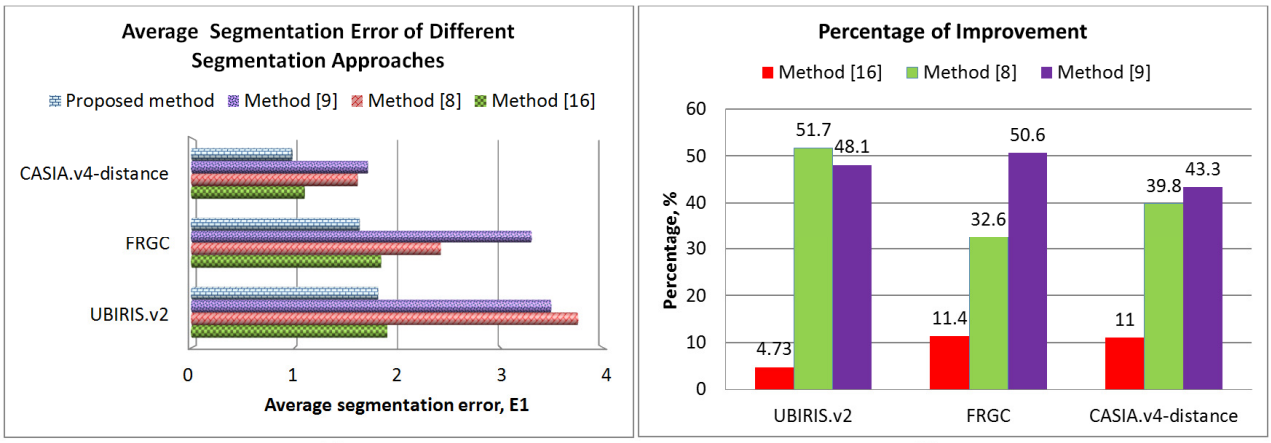

Figure 5: Segmentation performance. (a) Average segmentation error (E1), (b) Percentage of improvement. (*Best viewed in color*)

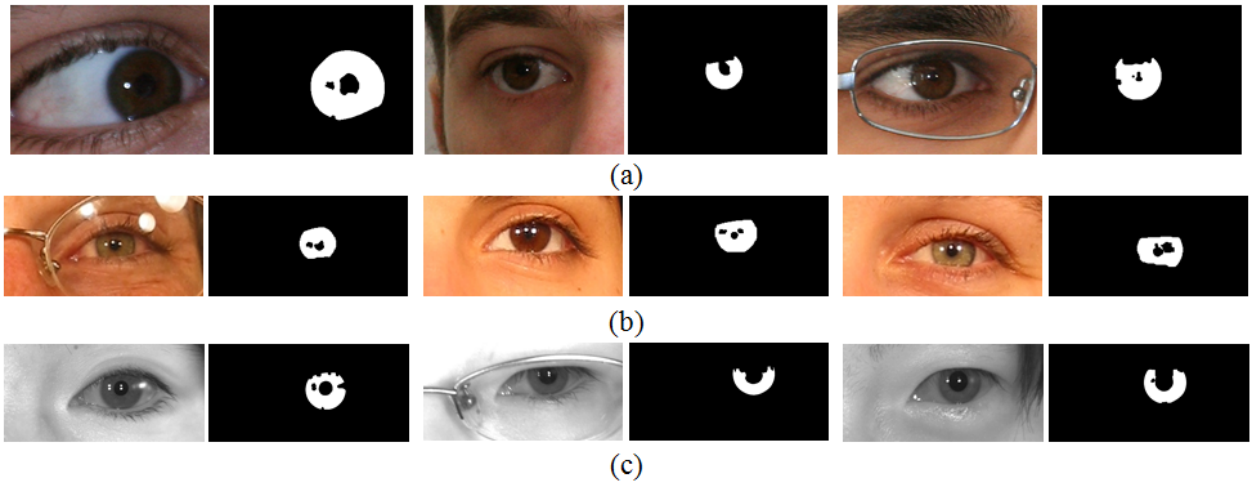

Figure 6: Sample segmentation results for (a) UBIRIS.v2, (b) FRGC, (c) CASIA.v4-distance databases.

3.1. Remotely acquired databases

In order to ascertain the performance of the developed iris segmentation approach, three publicly available databases which comprise of the images acquired using at-a-distance imaging were employed. Brief description of each database is provided below. The experimental results reported in this paper were obtained from the independent test images as summarized in following Table 1.

Table 1: Employed databases and respective train/test images.

	UBIRIS.v2	FRGC	CASIA.v4-distance
Imaging system	visible	visible	NIR
Acquisition distance (m)	4 - 8	N/A	≥3
No. of train images / subjects	96 / 19	40 / 13	79 / 10
No. of test images / subjects	904 / 152	500 / 150	502 / 67

- **UBIRIS.v2**: The full database consists of a total of 11102 images from 261 subjects. The images were acquired under unconstrained conditions with subjects at-a-distance and on-the-move. The stand-off distance (distance between subject and the camera) spanning from 4 to 9 meters. As similarly to [16], only subset of the images was employed in the experiment. The subset consists of 1000 images from 171 subjects. Images of the first 19 subjects were employed as training images for parameters training and the rest of 904 images were employed as test images.

- **FRGC**: The images from the high resolution still images category were considered in our experiments. As similar to [16], only subset of images was employed. The subset images were selected from the session 2002-269 to 2002-317 of Fall 2002. We employed the same procedure as reported in [16] for automatically localizing eye regions from these images using the AdaBoost eye detector [29-30].

- **CASIA.v4-distance**: The full database consists of a

Table 2: Summary of average execution time.

	Average Execution Time (second)	
	Method [16]	**Proposed method**
UBIRIS.v2	136.3	0.77
FRGC	51.1	0.16
CASIA.v4-distance	368.2	1.17

a total of 2567 images from 142 subjects. The images were acquired using NIR imaging with the subjects 3 meters away from the camera. Images from the first 10 subjects were employed as train images. For test images, images from the subjects 11 – 77 were employed in evaluating the segmentation performance. Note that only the *first eight left eye* images were considered in the experiments. Left eye regions were automatically extracted using the AdaBoost eye detector, as similar to the steps as also employed for the FRGC database.

3.2. Segmentation accuracy and complexity

Performance from the proposed iris segmentation method was evaluated using the protocol as adopted in the NICE.I competition [23]. The average segmentation error, $\overline{E_1}$ is given as follows:

$$\overline{E_1} = \frac{1}{N \times c \times r} \sum_{c' \in c} \sum_{r' \in r} O(c', r') \otimes C(c', r'), \qquad (3)$$

where O and C respectively correspond to the ground truth[1] and segmented iris masks, c and r denote the total numbers of columns and rows of the image; N is the total number of images. The XOR operator '$\otimes$' served to evaluate the disagreeing pixels between O and C.

It can be observed from the segmentation performance summarized in Figure 5 that the proposed approach outperforms the other methods [8, 9, 16] by achieving the average improvement of 34.8%, 31.5% and 31.4% in $\overline{E_1}$ on the three employed databases, respectively. By comparing to the best segmentation method among [8, 9, 16], the improvement of 4.73%, 11.4% and 11% are also observed, respectively for the UBIRIS.v2, FRGC and CASIA.v4-distance databases. Despite only the marginal improvement as compared to [16], the proposed segmentation approach provides a *significantly reduced computational cost* while performing effective iris segmentation, as can be observed from the average execution times summarized in Table 2. The approach detailed in [16] computed localized Zernike moment features for every image pixel, which may explains the reason why significant amount of time was dedicated. All the implementations were done in Matlab environment and executed on Intel Core i3 2.93GHz PC with 4GB RAM. Figure 6 illustrates some sample segmentation results obtained from the three employed databases.

[1] Ground truth masks for the three employed databases are publicly available at [17].

4. Conclusion and future work

This paper presented a computationally efficient iris segmentation approach which is developed based on the cellular automata. Our experimental results (table 2) have illustrated significant reduction in complexity of iris segmentation, especially for the images acquired under visible illumination, over the previously developed method in [16]. The computational simplicity of the developed approach significantly reduces the computational cost while providing comparable segmentation performance. As compared to the recently approaches [8, 9, 16], the proposed approach achieved average improvement of 34.8%, 31.5% and 31.4% in the average segmentation error which was obtained from the three publicly available databases, *i.e*. UBIRIS.v2, FRGC, and CASIA.v4-distance. The presented experimental results clearly demonstrate the superiority of the developed iris segmentation approach. In future work, we will focus in improving the accuracy of both iris segmentation and recognition for the distantly acquired visible illumination iris images. In this context, the sparse representation of local texture orientations can be employed as powerful feature extractor [34] and deserves further attention with future work involving at-a-distance iris images.

Acknowledgment

We thankfully acknowledge SOCIA Lab (University of Beira Interior, Portugal), NIST (USA) and Institute of Automation (Chinese Academy of Sciences, China) for their contributions to the databases employed in this work.

References

[1] J. Daugman and I. Malhas, "Iris recognition border-crossing system in the UAE," *International Airport Review*, 2004.

[2] K. Bowyer, K. Hollingsworth, and P. Flynn, "Image understanding for iris biometrics: A survey," *Image & Vision Computing*, vol. 110, no. 2, pp. 281–307, 2008.

[3] ISO/IEC 19794-6:2005. Information technology -- Biometric data interchange formats -- Part 6: Iris image data.

[4] J. Daugman, “How iris recognition works,” *IEEE Trans. Circuits Syst. & Video Technol.*, vol. 14, no. 1, pp. 21–30, 2004.

[5] R.P. Wildes, “Iris recognition: an emerging biometric technology,” *Proc. IEEE*, vol. 85, no. 9, pp.1348–1363, 1997.

[6] H. Proenca and L. Alexandre, “UBIRIS: A noisy iris image database,” *Proc. ICIAP 2005*, *Intl. Conf. Image Analysis & Processing*, vol. 1, 2005.

[7] H. Proenca, S. Filipe, R. Santos, J. Oliveira, and L. Alexandre, “The UBIRIS.v2: A database of visible wavelength images captured on the move and at-a-distance,” *IEEE Trans. Pattern Anal. Mach. Intell.*, vol. 32, no. 8, pp. 1529–1535, 2010.

[8] H. Proenca, “Iris recognition: On the segmentation of degraded images acquired in the visible Wavelength,” *IEEE Trans. Pattern Anal. Mach. Intell.*, vol. 32, no. 8, pp. 1502–1516, 2010.

[9] T. Tan, Z. He, and Z. Sun, “Efficient and robust segmentation of noisy iris images for non-cooperative iris recognition,” *Image & Vision Comput.*, vol. 28, no. 2, pp. 223–230, 2010.

[10] D. S. Jeong, J. W. Hwang, B. J. Kang, K. R. Park, C. S. Won, D.-K. Park and J. Kim, “A new iris segmentation method for non-ideal iris images,” *Image & Vision Comput.*, vol. 28, no. 2, pp. 254–260, 2010.

[11] P. Li, X. Liu, L. Xiao and Q. Song, “Robust and accurate iris segmentation in very noisy iris images,” *Image & Vision Comput.*, vol. 28, no. 2, pp. 246–253, 2010.

[12] W. Sankowski, K. Grabowski, M. Napieralska, M. Zubert and A. Napieralski, “Reliable algorithm for iris segmentation in eye image,” *Image & Vision Comput.*, vol. 28, no. 2, pp. 231–237, 2010.

[13] R. Donida Labati and F. Scotti, “Noisy iris segmentation with boundary regularization and reflections removal,” *Image & Vision Comput.*, vol. 28, no. 2, pp. 270–277, 2010.

[14] Y. Chen, M. Adjouadi, C. Han, J. Wang, A. Barreto, N. Rishe and J. Andrian, “A highly accurate and computationally efficient approach for unconstrained iris segmentation,” *Image & Vision Comput.*, vol. 28, no. 2, pp. 261–269, 2010.

[15] M. A. Luengo-Oroz, E. Faure and J. Angulo, “Robust iris segmentation on uncalibrated noisy images using mathematical morphology,” *Image & Vision Comput.*, vol. 28, no. 2, pp. 278–284, 2010.

[16] C.-W. Tan and A. Kumar, “A unified framework for automated iris segmentation using distantly acquired face images,” *IEEE Trans. Image Process*., available online, 2012.

[17] *Ground truth masks for iris segmentation*, http://www.comp.polyu.edu.hk/~csajaykr/myhome/research/GT.zip

[18] C.-W. Tan and A. Kumar, "Automated segmentation of iris images using visible wavelength face images," *Proc. CVPR 2011*, pp. 9–14, Colorado Springs, CVPRW'11, 2011.

[19] J. Daugman, “New methods in iris recognition,” *IEEE Trans. Syst. Man Cybern. Part B Cybern.*, vol. 37, no. 5, pp. 1167–1175, 2007.

[20] N. Kourkoumelis and M. Tzaphlidou, “Medical safety issues concerning the use of incoherent infrared light in biometrics,” in *Ethics and Policy of Biometrics* LNCS 6005, pp. 121–126, Springer Berlin / Heidelberg, 2010.

[21] Am. Nat’l Standards Inst. “American National Standard for the Safe Use of Lasers and LEDs Used in Optical Fiber Transmission Systems,” ANSI Z136.2, 1988.

[22] Commission Int’l de l’Eclarirage, “Photobiological Safety Standards for Safety Standards for Lamps,” Report of TC 6-38; CIE 134-3-99, 1999.

[23] NICE.I - Noisy Iris Challenge Evaluation, Part I. http://nice1.di.ubi.pt/index.html.

[24] NICE:II - Noisy Iris Challenge Evaluation, Part II. http://nice2.di.ubi.pt/.

[25] D. H. Brainard and B. A. Wandell, “Analysis of the retinex theory of color vision,” *J. Opt. Soc. Am. A:*, vol.3, no. 10, pp.1651–1661, 1986.

[26] V. Štruc and N. Pavešić, “Performance Evaluation of Photometric Normalization Techniques for Illumination Invariant Face Recognition,” *in Advances in Face Image Analysis: Techniques and Technologies*, Y. J. Zhang (*Ed.*), IGI Global.

[27] V. Štruc and N. Pavešić, “Gabor-Based Kernel Partial-Least-Squares Discrimination Features for Face Recognition,” *Informatica (Vilnius)*, vol. 20, no. 1, pp.115–138, 2009.

[28] V. Vezhnevets and V. Konouchine, “Grow-Cut - Interactive Multi-Label N-D Image Segmentation,” *Proc. Graphicon*, pp. 150–156, 2005.

[29] G. Bradski, “The OpenCV Library,” Dr. Dobb’s Journal of Software Tools, 2000.

[30] P. Viola and M. Jones, “Rapid object detection using a boosted cascade of simple features,” Proc. CVPR 2001, no., pp. 511–518, 2001.

[31] Face Recognition Grand Challenge – Overview. http://www.nist.gov/itl/iad/ig/frgc.cfm.

[32] P. Phillips, P. Flynn, T. Scruggs, K. Bowyer, J. Chang, K. Hoffman, J. Marques, J. Min, and W. Worek, “Overview of the face recognition grand challenge,” *in Computer Vision and Pattern Recognition, 2005. CVPR 2005*. 2005.

[33] Biometrics Ideal Test. http://biometrics.idealtest.org/dbDetailForUser.do?id=4.

[34] A. Kumar and T.-S. Chan, “Iris recognition using Quaternionic Sparse Orientation Code (QSOC),” *Proc. CVPR 2012*, Providence, Rhode Island, CVPRW’12, June 2012.